Contribution from the Department of Chemistry,
University of Minnesota, Minneapolis, Minnesota 55455

X-ray Crystal Structure and Homonuclear $^{31}P-^{31}P$ δ/J-Resolved NMR Spectroscopic Studies of $[AgIr_2(dimen)_4(PPh_3)_2](PF_6)_3$. Observation of a Statistical Mixture of "Head/Tail" Isomers

Andrew G. Sykes and Kent R. Mann*

Received October 16, 1989

The reaction of $[AgIr_2(dimen)_4(PF_6)_3$ (dimen = 1,8-diisocyanomenthane) with 2 equiv of triphenylphosphine results in the coordination of triphenylphosphine to the iridium atoms and forms a linear P–Ir–Ag–Ir–P unit. Recrystallization of the compound from acetone/hexane solutions afforded crystals of $[AgIr_2(dimen)_4(PPh_3)_2](PF_6)_3$ ($AgIr_2C_{84}H_{102}F_{18}N_8P_5$) that were the subject of X-ray structural characterization. The complex crystallizes in the monoclinic space group $C2/c$ (No. 15) with $Z = 4$, $a = 26.6$ (1) Å, $b = 4.67$ (1) Å, $c = 27.49$ (6) Å, $\beta = 117.8$ (3)°, and $V = 9496$ Å^3. At convergence, $R = 0.108$ and $R_w = 0.123$ for 1251 observed reflections. The structure features an encapsulated two-coordinate Ag^+ ion with Ir^+–Ag^+ distances of 2.642 (1) Å. The dimen ligands are disordered in a "head to tail" fashion about the iridium metal centers. Homonuclear $^{31}P\{^1H\}$ δ/J-resolved NMR data for solutions of the $[AgIr_2(dimen)_4(PPh_3)_2]^{3+}$ cation show that a statistical distribution of four different geometrical isomers with different "head to tail" orientations of the dimen ligand occurs in the complex.

Introduction

In a previous communication, we reported the reaction of silver ion with $[Ir_2(dimen)_4](PF_6)_2$[1] (dimen = 1,8-diisocyanomenthane, Figure 1), to form the $[AgIr_2(dimen)_4]^{3+}$ complex that features an encapsulated, two-coordinated Ag^+ ion. As was previously reported, encapsulation of the Lewis acid enhances the propensity of the complex to bind additional ligands (DMSO, PPh_3) in the axial iridium positions along the metal–metal bond axis of the molecule. The X-ray crystal structure of the DMSO adduct indicated that the dimen ligands are highly disordered in a "head to tail" manner, but we were unable to determine whether all the possible isomers are present in the solid or if a single, but disordered, isomer is present. Herein, we report the X-ray structure determination of the bis(triphenylphosphine) complex and $^{31}P\{^1H\}$ NMR solution studies, which have allowed us to determine the distribution of the unsymmetrical dimen ligands around the iridium metal centers.

Experimental Section

General Information. $[Ir_2(dimen)_4](PF_6)_2$ has previously been reported.[1,2] $AgPF_6$ and triphenylphosphine were purchased from Aldrich Chemical Co. All solvents were ACS reagent grade and were used without further purification in the synthesis. Elemental analyses were conducted by MHW Laboratories, Phoenix, AZ.

Properties of $[AgIr_2(dimen)_4(PPh_3)_2](PF_6)_3$. A 0.1047-g sample of $[Ir_2(dimen)_4(PF_6)_2$ (0.073 mmol) is dissolved in 10 mL of acetone. A slight excess of $AgPF_6$ (0.020 g, 0.080 mmol, 1.1 equiv) is added with rinsing, and the solution is allowed to sit with no stirring for approximately 0.5 h until the purple $[Ir_2(dimen)_4](PF_6)_2$ has faded to the yellow color of the encapsulated Ag adduct. A 0.0431-g amount of triphenylphosphine (0.165 mmol, 2.2 equiv) is added, and the color immediately changes to a pale yellow. This solution is rotovapped to one-fourth the original volume and the product precipitated by addition of 50 mL of hexane. The product is collected on a fritted glass funnel, washed with hexanes, and dried under vacuum.

Characterization of $[Ir_2Ag(dimen)_4(PPh_3)_2](PF_6)_3$. ^1H NMR (300 MHz, CD_3CN, 25 °C), δ: phenyl 7.579 (m, 18 H), 7.382 (m, 12 H); dimen methyls 1.329, 1.284, 1.256, 1.240, 1.219 (36 H); dimen methylene and methine protons observed as multiplets between 2.060 and 1.031. Integration confirmed the number of protons due to each observed resonance. $^{13}C\{^1H\}$ NMR (75.7 MHz, acetone-d_6, 25 °C), δ: phenyl 133.51, 132.34, 130.38; dimen 1-C 63.71, 2,6-C 38.16, 3,5-C 24.14, 4-C 46.20, 7-C 28.20, 8-65.59, 9,10-C 27.78; isocyanide carbons not observed. Assignment of signals was based on (*Z*)-1,8-diamino-*p*-menthane:[3] $^{31}P\{^1H\}$ NMR (121.5 MHz, CH_2Cl_2, 25 °C) δ −14.6 (m) vs external H_3PO_4; IR (CH_2Cl_2) ν(CN) = 2184 cm^{-1}; UV/vis (CH_3CN) λ_{max} = 340 nm, ϵ_{max} = 4.1 × 10^4 cm^{-1}; FAB-MS *m/e* for $\{[Ir_2Ag(dimen)_4(PPh_3)_2](PF_6)_2\}^+$ calcd 2067.53, found 2067.1 (theoretical and experimental isotopic intensities and distribution in close agreement). Anal. Calcd for $AgIr_2C_{84}H_{102}F_{18}N_8P_5$: C, 45.60; H, 4.61; N, 5.07. Found: C, 45.45; H, 4.73; N, 5.16.

* To whom correspondence should be addressed.

Table I. Crystallographic Data and Collection Parameters for $[AgIr_2(dimen)_4(PPh_3)_2](PF_6)_3$

$AgIr_2C_{84}H_{102}F_{18}N_8P_5$	2212.93
a = 26.6 (1) Å	space group $C2/c$ (No. 15)
b = 14.67 (1) Å	T = −80 °C
c = 27.49 (6) Å	μ = 0.710 71 Å
α = 90°	σ = 1.548 g/cm^3
β = 117.8 (3)°	μ = 31.5 cm^{-1}
γ = 90°	transm coeff = 1
V = 9496 Å^3	R = 0.108
Z = 4	R_w = 0.123

Instrumentation. IR spectra were obtained with a Perkin-Elmer 1710 infrared FT spectrometer, and UV/vis spectra were obtained with a Cary 17-D spectrophotometer interfaced to a Zenith 150 microcomputer.

^1H and ^{13}C NMR spectra were recorded at 300 and 75.7 MHz, respectively, with Nicolet NT-300WB and IBM AC-300 spectrometers. Chemical shifts were referenced to the residual proton or carbon resonances of the solvent. All chemical shifts are reported in units of δ. ^{31}P NMR spectra were recorded on the Nicolet NT-300WB, and the chemical shifts were referenced to external phosphoric acid run prior to the samples. NMR simulations were conducted with a Zenith 150 microcomputer using the RACCOON program.[4]

Fast atom bombardment (FAB) mass spectra were obtained with a VG Analytical VG 7070E-HF high-resolution double-focusing mass spectrometer equipped with a VG 11/250 data system. Spectra were obtained at a resolution of 1 part in 2000. Ions were generated by bombardment of the target matrix with a neutral xenon atom beam (derived from a Xe^+ ion beam accelerated at 8 kV). Samples for FAB mass spectroscopy were prepared by dissolving the complexes in *m*-nitrobenzoic acid. Simulations of the isotopic distribution patterns were carried out with a program provided with the VG 7070E-HF instrument.

$^{31}P-^{31}P$ δ/J-Resolved NMR Spectroscopy. FID's were collected with the pulse sequence $90°-\tau_1-180°-\tau_1-\text{echo}(\tau_2)$.[5] The evolution time t_1 considered as $2\tau_1$ (i.e. the time between the onset of the 90° pulse and the acquisition) ranged incrementally from 5 to 640 ms. Fourier transformation in both time domains (t_2 was the elapsed time of recording the FID) gave a two-dimensional spectrum in two frequency dimensions, f_1 and f_2. Fourier transformation with respect to f_2 gave both chemical shift and coupling information, while f_1 yielded the values of coupling constants only, with the splitting pattern centered at zero. Because t_1 causes modulation in the FID due to P–P coupling constants, separation of the chemical shift and coupling constant information results from a 45° "tilting" of f_2. The two-dimensional series of spectra represent a plot of $^{31}P\{^1H, ^{31}P-^{31}P\}$-decoupled chemical shifts (f_2) vs P–P couplings (f_1). Resolution in the two-dimensional spectrum is 2.7 Hz/point in the f_2

(1) Sykes, A.; Mann, K. R. *J. Am. Chem. Soc.* **1988**, *110*, 8252.
(2) Smith, T. P. Ph.D. Thesis, California Institute of Technology, 1982.
(3) Liptak, A.; Kusiak, J. W.; Pitha, J. *J. Med. Chem.* **1985**, *28*, 1699.
(4) RACCOON was written for the IBM microcomputer by P. F. Schatz.
(5) (a) Aue, W. P.; Karhan, J.; Ernst, R. R. *J. Phys. Chem.* **1976**, *64*, 4266. (b) Aue, W. P.; Bartholdi, E.; Ernst, R. R. *J. Chem. Phys.* **1976**, *64*, 2229.

0020-1669/90/1329-4449$02.50/0

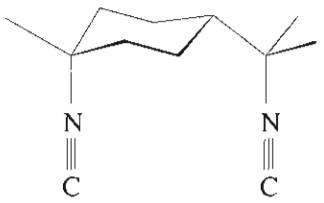

Figure 1. Representation of the 1,8-diisocyano-*p*-menthane ligand.

dimension and 1.56 Hz/point in the f_1 dimension, leaving an approximate ±3-Hz error in the chemical shift and coupling data.

X-ray Data Collection and Reduction. A small white crsytal of $[AgIr_2(dimen)_4(PPh_3)_2](PF_6)_3$ of unknown physical dimensions was obtained by slow diffusion of hexane into a concentrated acetone solution containing the complex. Crystal data are tabulated in Table I. Because of the small size of the crystal, reliable intensities could not be collected for $\theta > 16°$. Repeated attempts to grow larger crystals were unsuccessful. The automatic peak searching, centering, and indexing routines available on the Enraf-Nonius SDP-CAD4 automatic diffractometer[6] were used to find and center the reflections that were used to define the unit cell parameters. Cell constants were obtained from a least-squares refinement of the setting angles of 10 carefully centered reflections in the range $12.00 < 2\theta < 27.00°$. Systematic absences ($hk1$, $h + k \neq 2n$; $h0l$, $l \neq 2n$) and refinement of the structure identified the space group as $C2/c$ (No. 15).

Data processing and reduction,[7] Patterson function, Fourier and difference Fourier syntheses, and least-squares refinement[8] were carried out with the computer programs available in the Enraf-Nonius structure-solving package. Scattering factors were from Cromer and Waber[9] and included the effects of anomalous dispersion.[10,11] All calculations were performed by using the TEXSAN[12] crystallographic software package of the Molecular Structure Corp. The intensities of three representative reflections that were measured after every 50 min of X-ray exposure time remained constant throughout the data collection, indicating crystal and electronic stability. No decay or absorption corrections were applied. Azimuthal scans of several reflections indicated no need for an absorption correction. The data were corrected for Lorentz and polarization effects.

Structure Solution and Refinement. The heavy-atom positions were found from a Patterson map.[13] The phosphorus atoms and approximately half of the light atoms were found from a series of Fourier and difference Fourier maps. One of the phenyl rings in the triphenylphosphine ligand, the PF_6^- anions, and the dimen ligands appeared to be disordered. The phenyl rings, PF_6, and the dimen ligands were subject to further refinement as rigid groups (Table II contains a list of final coordinates). This produced a cation with reasonable parameters; however, the only bond lengths and bond angles of the structure we regard with confidence are those involving the Ag, Ir, and ligand P atoms.

Results and Discussion

The addition of 2 equiv of triphenylphosphine to a solution of $[AgIr_2(dimen)_4](PF_6)_3$ in acetone gives white $[AgIr_2(dimen)_4(PPh_3)_2](PF_6)_3$ in quantitative yield. Slow recrystallization from acetone/hexane solutions gave colorless crystals that were the subject of an X-ray structural characterization. A PLUTO[14] illustration of the $[AgIr_2(dimen)_4(PPh_3)_2]^{3+}$ cation is shown in Figure 2.

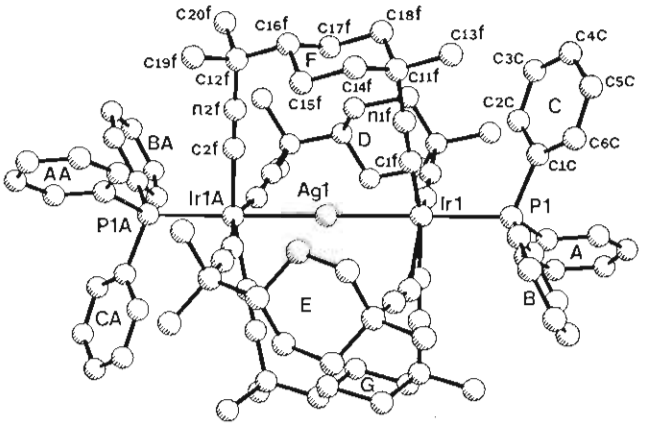

Figure 2. PLUTO[19] diagram of the $[AgIr_2(dimen)_4(PPh_3)_2]^{3+}$ cation that illustrates the numbering scheme. Triphenylphosphine rings are labeled with the suffixes A, B, and C and (for the symmetry-related group) AA, BA, and CA. The dimen ligands are indicated with the D, E, F, and G suffixes.

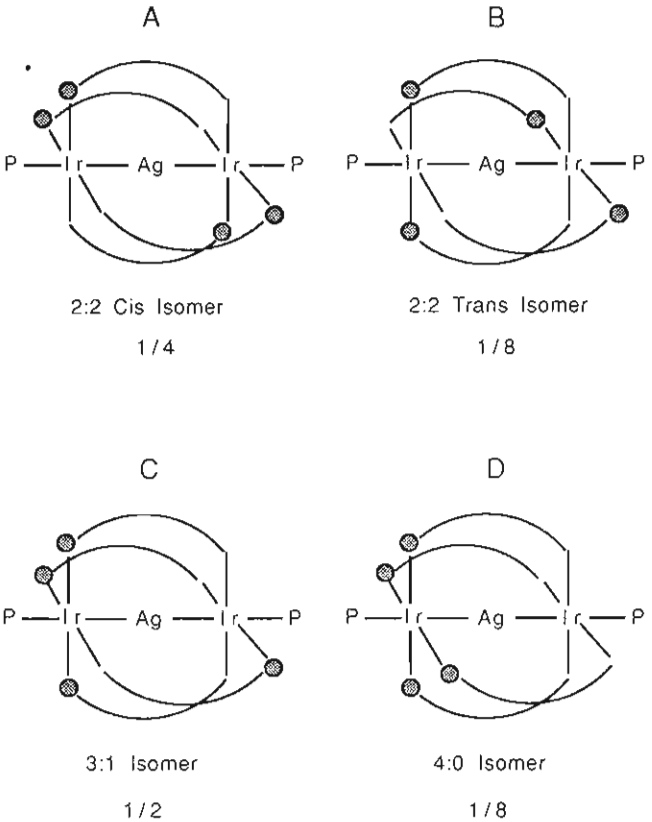

Figure 3. Schematic representations of the four geometric isomers, A–D, which include the P–Ir–Ag–Ir–P backbone and possible distributions of four unsymmetrical 1,8-diisocyanomenthane ligands. The fraction indicates the statistical amount expected for each isomer.

The Ag^+ ion remains encapsulated by the Ir_2^{2+} complex, and the two triphenylphosphine ligands are bound to iridium in the axial positions trans to the Ir–Ag bonds to form a nearly collinear P–Ir–Ag–Ir–P^{3+} unit. The Ir–Ag–Ir bond angle of 180° and the Ir–Ag distances of 2.64 (1) Å require an interatomic distance of 5.28 (1) Å between the iridium atoms. Ir–P bond distances are 2.39 (3) Å, and the P–Ir–Ag bond angles are 174 (1)°. The P–Ir–Ag–Ir–P^{3+} unit compares very favorably with the S–Ir–

(6) All calculations were carried out on PDP 8A and 11/34 computers using the Enraf-Nonius CAD4-SDP programs.
(7) The intensity data are processed as described previously: Bohling, D. A.; Mann, K. R. *Inorg. Chem.* **1984**, *23*, 1426.
(8) Function minimized $\sum w(|F_o| - |F_c|)^2$, where $w = 4F_o^2/\sigma^2(F_o^2)$ and $\sigma^2(F_o^2) = [S^2(C + R^2B) + (pF_o^2)^2]/(Lp)^2$ (S = scan rate, C = total integrated peak count, R = ratio of scan time to background counting time, B = total background count, Lp = Lorentz-polarization factor, P = P factor). The final R index $(\sum||F_o| - |F_c||/\sum|F_o|) = 0.108$, and the weighted agreement factor R_w $([(\sum w(|F_o| - |F_c|)^2/\sum wF_o^2)]^{1/2}) = 0.123$. The standard deviation of an observation of unit weight[14] was 2.64. Standard deviation of an observation of unit weight was $[\sum w(|F_o| - |F_c|)^2/(NO - NV)]^{1/2}$, where NO = number of observations, NV = number of variables.
(9) Cromer, D. T.; Waber, J. T. *International Tables for X-ray Crystallography*; The Kynoch Press: Birmingham, England, 1974; Vol. IV, Table 2.2 A.
(10) Ibers, J. A.; Hamilton, W. C. *Acta Crystallogr.* **1964**, *17*, 781.
(11) Cromer, D. T. *International Tables for X-ray Crystallography*; The Kynoch Press: Birmingham, England, 1974; Vol. IV, Table 2.3.1.
(12) *TEXSAN-TEXRAY Structure Analysis Package*; Molecular Structure Corp.: Woodlands, TX, 1985.
(13) Calbrese, J. C. PHASE: Patterson Heavy Atom Solution Extractor. Ph.D. Thesis, University of Wisconsin—Madison, 1972.
(14) Motherwell, S.; Clegg, W. PLUTO: program for plotting molecular and crystal structures. University of Cambridge, England, 1978.

Table II. Positional Parameters[a] and Their Estimated Standard Deviations for $[AgIr_2(dimen)_4(PPh_3)_2](PF_6)_3$

atom	x	y	z	B, Å²	atom	x	y	z	B, Å²
Ag1	0.2500 (0)	0.2500 (0)	0.0000 (0)	4.1 (4)	C1D	0.224 (3)	0.054 (4)	−0.012 (3)	7 (1)
Ir1	0.2290 (2)	0.1121 (2)	0.0496 (1)	6.3 (2)	C2D	0.276 (2)	0.248 (3)	−0.127 (2)	7 (1)
P1	0.205 (1)	−0.020 (2)	0.0850 (9)	8.4 (6)	C2D	0.264 (3)	0.306 (3)	−0.106 (3)	7 (1)
P2	0.631 (1)	0.139 (2)	0.175 (1)	23 (1)	C11E	0.190 (4)	0.330 (6)	0.155 (3)	20 (3)
F21	0.661 (2)	0.161 (3)	0.236 (1)	23 (1)	C12E	0.266 (4)	0.536 (5)	0.095 (4)	20 (3)
F22	0.687 (1)	0.153 (3)	0.173 (2)	23 (1)	C14E	0.157 (4)	0.418 (6)	0.130 (4)	20 (3)
F23	0.617 (2)	0.240 (2)	0.162 (2)	23 (1)	C15E	0.180 (3)	0.465 (5)	0.095 (4)	20 (3)
F24	0.645 (2)	0.038 (2)	0.188 (2)	23 (1)	C16E	0.243 (4)	0.489 (5)	0.131 (3)	20 (3)
F25	0.575 (1)	0.126 (4)	0.177 (2)	23 (1)	C17E	0.277 (3)	0.400 (6)	0.155 (3)	20 (3)
F26	0.601 (2)	0.117 (3)	0.113 (1)	23 (1)	C18E	0.254 (4)	0.353 (7)	0.191 (3)	20 (3)
P3	0.496 (3)	0.423 (3)	0.748 (3)	19 (2)	C19E	0.233 (5)	0.624 (5)	0.071 (5)	20 (3)
F31	0.557 (3)	0.462 (5)	0.772 (4)	19 (2)	C20E	0.329 (4)	0.559 (7)	0.131 (5)	20 (3)
F32	0.481 (4)	0.468 (4)	0.693 (3)	19 (2)	N1E	0.182 (4)	0.263 (5)	0.113 (4)	20 (3)
F33	0.477 (4)	0.509 (4)	0.767 (3)	19 (2)	C1E	0.175 (5)	0.209 (6)	0.080 (5)	20 (3)
F34	0.516 (4)	0.337 (4)	0.730 (4)	19 (2)	N2E	0.263 (5)	0.483 (7)	0.049 (4)	20 (3)
F35	0.512 (4)	0.378 (4)	0.804 (3)	19 (2)	C2E	0.260 (6)	0.441 (8)	0.013 (5)	20 (3)
F36	0.436 (3)	0.384 (5)	0.725 (4)	19 (2)	C11F	0.408 (2)	0.098 (3)	0.161 (2)	4.9 (9)
C1A	0.152 (2)	−0.095 (4)	0.034 (3)	10 (1)	C12F	0.457 (2)	0.317 (3)	0.084 (2)	4.9 (9)
C2A	0.142 (2)	−0.176 (5)	0.055 (2)	10 (1)	C13F	0.413 (3)	0.020 (3)	0.200 (2)	4.9 (9)
C3A	0.104 (3)	−0.241 (3)	0.019 (3)	10 (1)	C14F	0.434 (2)	0.185 (3)	0.195 (1)	4.9 (9)
C4A	0.076 (2)	−0.224 (4)	−0.038 (3)	10 (1)	C15F	0.429 (2)	0.264 (2)	0.155 (1)	4.9 (9)
C5A	0.086 (2)	−0.142 (5)	−0.058 (2)	10 (1)	C16F	0.462 (1)	0.238 (3)	0.123 (2)	4.9 (9)
C6A	0.124 (3)	−0.078 (3)	−0.022 (3)	10 (1)	C17F	0.436 (2)	0.151 (2)	0.090 (2)	4.9 (9)
C1B	0.182 (3)	0.008 (3)	0.138 (2)	10 (1)	C18F	0.441 (2)	0.073 (2)	0.129 (2)	4.9 (9)
C2B	0.125 (3)	−0.001 (3)	0.125 (2)	10 (1)	C19F	0.483 (2)	0.404 (3)	0.118 (2)	4.9 (9)
C3B	0.105 (2)	0.030 (4)	0.161 (3)	10 (1)	C20F	0.490 (2)	0.291 (3)	0.052 (2)	4.9 (9)
C4B	0.143 (3)	0.071 (3)	0.211 (2)	10 (1)	N1F	0.348 (2)	0.106 (3)	0.125 (2)	4.9 (9)
C5B	0.200 (3)	0.081 (3)	0.224 (2)	10 (1)	C1F	0.300 (2)	0.1123 (4)	0.0997 (2)	4.9 (9)
C6B	0.220 (2)	0.049 (4)	0.188 (3)	10 (1)	N2F	0.400 (2)	0.340 (3)	0.043 (2)	4.9 (9)
C1C	0.266 (2)	−0.093 (4)	0.125 (5)	16 (2)	C2F	0.354 (2)	0.358 (3)	0.011 (2)	4.9 (9)
C2C	0.297 (5)	−0.109 (5)	0.096 (2)	16 (2)	C11G	0.058 (4)	0.210 (5)	−0.018 (3)	19 (2)
C3C	0.344 (4)	−0.165 (6)	0.118 (4)	16 (2)	C12G	0.079 (4)	0.440 (5)	−0.107 (3)	19 (2)
C4C	0.362 (2)	−0.206 (4)	0.169 (5)	16 (2)	C13G	0.030 (5)	0.142 (7)	0.005 (4)	19 (2)
C5C	0.332 (5)	−0.191 (5)	0.198 (2)	16 (2)	C14G	0.028 (3)	0.206 (6)	−0.081 (3)	19 (2)
C6C	0.284 (4)	−0.134 (6)	0.176 (4)	16 (2)	C15G	0.056 (3)	0.274 (5)	−0.103 (2)	19 (2)
C11D	0.257 (2)	−0.048 (3)	−0.070 (2)	7 (11)	C16G	0.051 (3)	0.371 (5)	−0.084 (3)	19 (2)
C12D	0.292 (2)	0.176 (3)	−0.153 (2)	7 (1)	C16G	0.081 (4)	0.375 (4)	−0.021 (3)	19 (2)
C13D	0.251 (3)	−0.145 (3)	−0.052 (3)	7 (1)	C18G	0.9053 (4)	0.307 (6)	0.001 (3)	19 (2)
C14D	0.319 (2)	−0.030 (3)	−0.056 (2)	7 (1)	C19G	0.949 (5)	0.436 (7)	−0.170 (3)	19 (2)
C15D	0.325 (2)	0.068 (3)	−0.074 (2)	7 (1)	C20G	0.074 (5)	0.537 (4)	−0.088 (4)	19 (2)
C16D	0.286 (2)	0.079 (3)	−0.136 (2)	7 (1)	N1G	0.116 (4)	0.179 (5)	0.006 (3)	19 (2)
C17D	0.224 (2)	0.061 (3)	−0.149 (2)	7 (1)	C1G	0.162 (4)	0.154 (6)	0.025 (4)	19 (2)
C18D	0.218 (2)	−0.037 (3)	−0.132 (2)	7 (1)	N2G	0.139 (4)	0.424 (5)	−0.089 (3)	19 (2)
C19D	0.354 (2)	0.194 (4)	−0.140 (3)	7 (1)	C2G	0.186 (4)	0.412 (7)	−0.076 (4)	19 (2)
C20D	0.253 (3)	0.187 (4)	−0.216 (2)	7 (1)					
N1D	0.239 (2)	0.009 (4)	−0.037 (2)	7 (1)					

[a] Suffixes A, B, and C refer to phenyl rings of the PPh_3 ligand while D, E, F, and G refer to the four dimen ligands.

Ag–Ir–S^{3+} unit observed in the X-ray structural characterization of $[AgIr_2(dimen)_4(DMSO)_2](PF_6)_3$.[1] The Ir–Ag distances for the $[AgIr_2(dimen)_4(DMSO)_2]^{3+}$ cation are 2.642 (1) Å, identical with those of the phosphine-containing adduct, and the values of 179.97 (3) and 170.41 (13)° for the Ir–Ag–Ir and S–Ir–Ag bond angles, respectively, compare closely to analogous parameters in the phosphine structure. A slight difference is observed in the shorter Ir–P distance of 2.39 (3) Å compared with the Ir–S distance of 2.458 (6) Å.

Although the X-ray structures of the linear core are similar, the isocyanide stretching frequencies observed in the infrared spectra of the two complexes suggest some significant changes in the electron density at Ir. $[AgIr_2(dimen)_4(PPh_3)_2]^{3+}$ has a single ν(CN) stretch at 2184 cm^{-1} (solution spectra, CH_2Cl_2), whereas $[AgIr_2(dimen)_4(DMSO)_2]^{3+}$ has a single stretch 12 cm^{-1} higher in energy at 2196 cm^{-1} (neat DMSO). We believe that the σ donor, triphenylphosphine, increases the electron density at iridium, increases back-bonding to the isocyanides, and decreases the bond order of the CN bond to lower the IR stretch. Dissolution of the Ir–Ag–Ir^{3+} cation in other coordinating solvents also produces changes in the CN stretching frequency. The solvents acetone and acetonitrile give intermediate stretching frequences (2190 and 2191 cm^{-1}, respectively).

The binding of triphenylphosphine along the Ir–Ag–Ir axis of the encapsulated silver adduct has provided an excellent tool for investigating the distribution of the unsymmetrical dimen ligands around the iridium metal centers. The one-dimensional $^{31}P\{^1H\}$ NMR spectrum of $[AgIr_2(dimen)_4(PPh_3)_2](PF_6)_3$ reveals the typical PF_6^- septet at −144 ppm and a complex multiplet for the coordinated PPh_3 ligands at −14.7 ppm (Figure 4C). The complexity of the −14.7 ppm signal indicates that it is likely due to a mixture of geometric isomers produced by the consecutive addition of four unsymmetrical dimen ligands in the synthesis of the iridium binuclear parent complex, $[Ir_2(dimen)_4](PF_6)_2$. After the terminal phosphines are bound to the silver adduct, four isomers, A–D (shown in Figure 3), are possible. If these isomers are formed in the statistical amounts, they would be present in the relative ratios $^1/_8$, $^1/_2$, $^1/_8$, respectively. The solid circle of the schematically depicted dimen ligand represents the dimethyl-substituted quaternary carbon end of the diisocyanide ligand. The 2:2 cis isomer, A, has two chemically equivalent axial phosphorus atoms, as does the 2:2 trans isomer (B), but the two isomers have different ^{31}P chemical shifts. The 3:1 and 4:0 isomers, C and D, have inequivalent axial positions due to either three or four dimen ligands, with the dimethyl-substituted ends on one iridium and one or no dimethyl-substituted end on the other iridium, respectively. These two isomers (C and D) have unique chemical shifts for each of the phosphorus atoms. Thus, the complex overlapping multiplet observed in the one-dimensional ^{31}P spectrum at −14.7 ppm is the sum of six phosphorus signals of the four different isomers coupled in all instances to either ^{109}Ag or ^{107}Ag. Additionally, in the case of the 3:1 and 4:0 isomers,

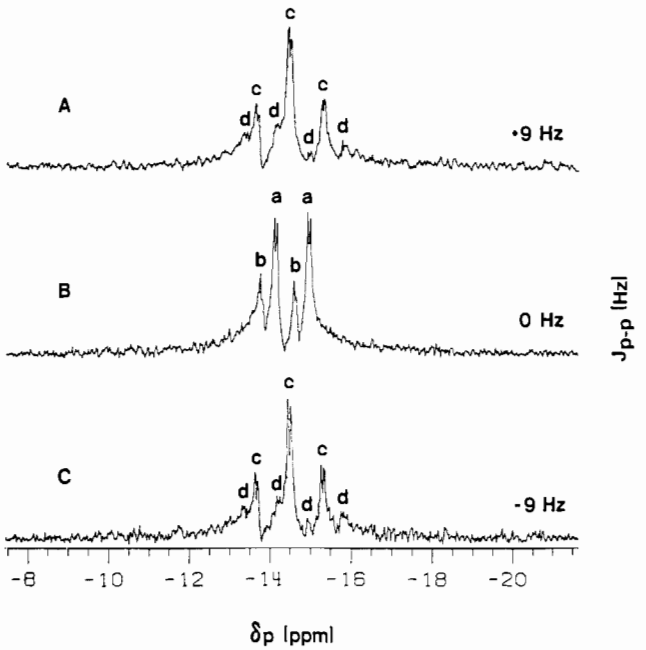

Figure 4. (A) Individually simulated contributions of isomers A–D. (B) Spectrum simulated by using a line-broadening of 3.5 Hz and the spectral parameters reported in Table III. (C) One-dimensional 121.5-MHz $^{31}P\{^1H\}$ spectrum of a ca. 50 mM solution of $[AgIr_2)(dimen)_4(PPh_3)](PF_6)_3$ in CD_2Cl_2 taken at 27 °C. The PF_6^- septet has been omitted.

Table III. ^{31}P NMR Data for $[AgIr_2(dimen)_4(PPh_3)_2](PF_6)_3$

isomer	chem shift ppm	coupling const, Hz		
		$J_{^{109}Ag-P}$	$J_{^{107}Ag-P}$	J_{P-P}
A	−14.77	105.3	94.3	
B	−14.45	106.4	93.9	
C	−14.30	105.7	94.3	21
	−15.10			
D	−14.10	106.0	94.0	21
	−15.60			

where the ^{31}P atoms are chemically nonequivalently, the terminal phosphines are expected to be observably coupled to each other.

The complexity of the one-dimensional ^{31}P multiplet suggested that we investigate the applicability of two-dimensional δ/J-resolved spectroscopy[4] to simplify the complex ^{31}P pattern. Heteronuclear two-dimensional δ/J-resolved spectroscopy has frequently been useful in understanding complex ^1H and ^{13}C NMR spectra,[5b] but homonuclear two-dimensional δ/J-resolved spectroscopy has been limited primarily to the study of ^1H systems.[15] Homonuclear δ/J-resolved two-dimensional ^{31}P spectroscopy has been almost exclusively limited to a few organophosphorus compounds[16] and a few phosphorus-containing transition-metal complexes.[17]

Figure 5 shows three slices of the 45°-tilted, 121.5-MHz, two-dimensional $^{31}P\{^1H\}$ δ/J-resolved spectrum of $[AgIr_2(dimen)_4(PPh_3)_2]^{3+}$. The f_2 axis exhibits phosphorus-decoupled chemical shift data and heteroatom coupling to ^{107}Ag and ^{109}Ag. P–P coupling constants are read directly off the f_1 axis as an initial starting point for simulating the one-dimensional ^{31}P spectrum.

The observed spectra (Figure 4) are in close agreement with those simulated with the spectral constants listed in Table III.

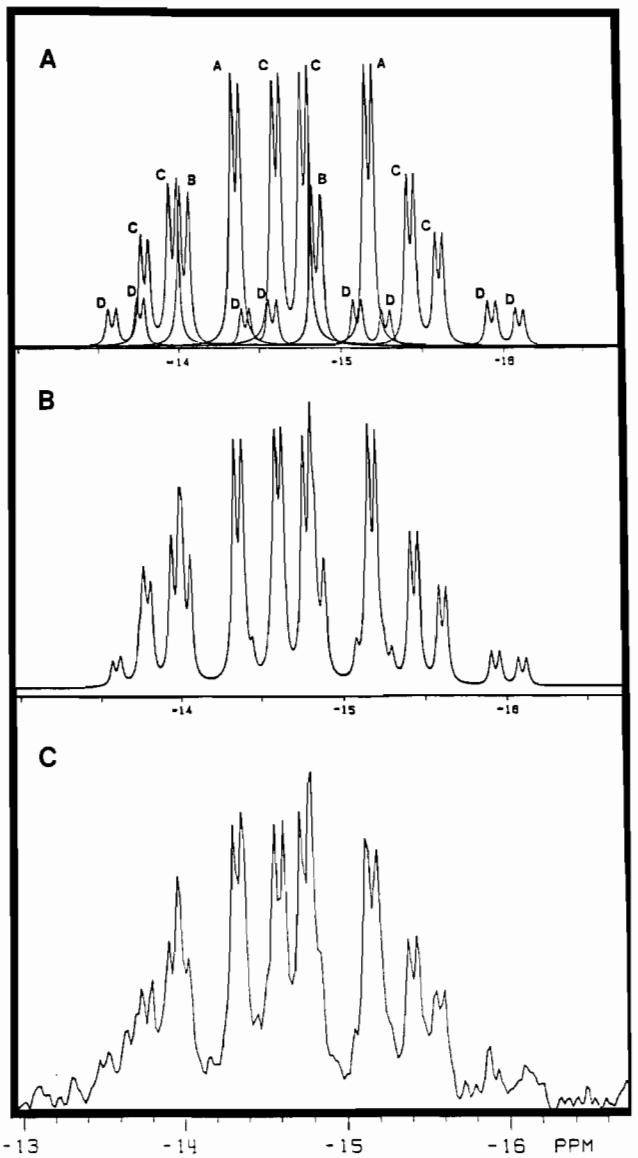

Figure 5. Three slices of the 45°-tilted, homonuclear δ/J-resolved two-dimensional ^{31}P NMR spectrum recorded at 121.5 MHz with broad-band decoupling of proton nuclei on a Nicolet NT-300WB spectrometer. Spectrum B shows the phosphorus signals of isomers A and B exhibiting coupling to only ^{107}Ag and ^{109}Ag. Spectra A and C are the phosphorus-decoupled signals for isomers C and D (heteronuclear Ag–P coupling included with approximate 18-Hz P–P coupling given on the J_{P-P} axis). A data matrix of 128 × 1024 points was acquired in the (τ_1, τ_2) domains, and four transients for each value of τ_1 gave a sufficient signal-to-noise ratio.

The line intensities found for $J = 0$ in Figure 5 represent phosphorus nuclei with no observable P–P coupling. We attribute these peaks to isomers A and B (2:1 ratios), which have equivalent axial phosphines. The larger doublet of doublets is due to isomer A. The doublet of doublets pattern is the result of ^{107}Ag–P and ^{109}Ag–P coupling in the different molecules. ^{107}Ag and ^{109}Ag occur in 51.35 and 48.65% natural abundance, and both have $I = {}^1/_2$. ^{109}Ag is responsible for the larger coupling, and the ratio of ^{109}Ag–P to ^{107}Ag–P coupling is theoretically equal to 1.149, the ratio of their gyromagnetic moments.[18] The average ^{109}Ag–P coupling constant for isomers A–D is 106 Hz, and ^{107}Ag–P coupling averages 94 Hz to give a ^{109}Ag–P:^{107}Ag–P ratio of 1.13, in good agreement with the theoretical prediction.

The unsymmetrical arrangement of dimen ligands around the two iridium metal centers in isomers C and D creates inequivalent

(15) (a) Nagayama, K.; Wuthrich, K.; Bachmann, P.; Ernst, R. R. *Biochem. Biophys. Res. Commun.* **1977**, *78*, 99. (b) Nagayama, K.; Bachmann, P.; Wuthrich, K.; Ernst, R. R. *J. Magn. Reson.* **1978**, *31*, 133.

(16) Colquhoun, I. J.; McFarlane, W. *J. Chem. Soc., Chem. Commun.* **1982**, 484.

(17) (a) Chiu, K. W.; Rzepa, H. S.; Sheppard, R. N.; Wilkinson, G.; Wong, W. K. *J. Chem. Soc., Chem. Commun.* **1982**, 482. (b) Chiu, K. W.; Howard, C. G.; Rzepa, H. S.; Sheppard, R. N.; Wilkinson, G.; Galas, A. M. R.; Hursthouse, M. B. *Polyhedron* **1982**, *1*, 441. (c) Chiu, K. W.; Rzepa, H. S.; Sheppard, R. N.; Wilkinson, G.; Wong, W. K. *Polyhedron* **1982**, *1*, 809.

(18) (a) Muetterties, E. L.; Alegranti, C. W. *J. Am. Chem. Soc.* **1970**, *92*, 4114. (b) Muetterties, E. L.; Alegranti, C. W. *J. Am. Chem. Soc.* **1972**, *94*, 6386.

terminal phosphorus environments. Two chemical shifts and observable P–P coupling for each isomer result. In isomer C, $\Delta\delta$ for the inequivalent phosphorus atoms and the average Ag–P coupling constants are both approximately equal to 100 Hz and combine to produce a pair of overlapping doublet of doublets, which appear as a triplet pattern (Figure 5, J = +9 or −9 Hz). Isomer D has ^{31}P chemical shifts more disparate in magnitude ($\Delta\delta$ is approximately 180 Hz with Ag–P coupling of 100 Hz), and the expected doublet of doublets of doublets pattern is observed. The 18-Hz phosphorus–phosphorus coupling constant is read directly from the f_1 axis (Figure 5). The less precise P–P coupling constant value is almost identical for isomers C and D and is within experimental error of the 21-Hz value used to simulate both isomers in the one-dimensional spectrum.

The 100-Hz two-bond Ag–P coupling constants are larger than two-bond couplings found in similar compounds.[19] Two-bond couplings between Ag and a phosphine on a heteroatom are generally unresolved, and the average Ag–P couplings are ca. 8–32 Hz. The 21-Hz P–P coupling in the 3:1 and 4:0 isomers is also high for a four-bond coupling.[20] The large through-metal Ag–P and P–P coupling constants in $[AgIr_2(dimen)_4(PPh_3)_2](PF_6)_3$ are likely due to the high symmetry of the complex, the coordination number of 2 for Ag^+, and the collinear nature of the P–Ir–Ag–Ir–P^{3+} bond vectors.

The chemical shifts of isomer A–D (the 2:2 cis and trans isomers) of −14.77 and −14.45 ppm, respectively, are close to the average of the two phosphorus chemical shifts in the 3:1 (−14.7 ppm) and 4:0 (−14.85 ppm) isomers. It is useful to realize that as the dimen ligands in the 2:2 isomers are reversed one by one to yield first the 3:1 and then the 4:0 isomer, the chemical shifts of the inequivalent phosphorus atoms diverge. One end of the P–Ir–Ag–Ir–P unit progressively becomes more crowded as the bulkier dimethyl-substituted ends of the dimen ligands bind to the same side of the molecule. In the extreme case of the 4:0 isomer, one terminal phosphine ligand is adjacent to four methyl groups while the other terminal phosphine ligand is exposed to eight methyl groups.

The interconversion rate of the four isomers is slow on the ^{31}P NMR time scale. The sharpness of the individual peaks in the complex multiplet at −14.7 ppm indicates that fluxional processes which involve the dissociation of triphenylphosphine from the axial positions are slow. The compound is robust in solution, and no free triphenylphosphine is observed in the ^{31}P NMR spectrum. When 1 additional equiv of triphenylphosphine is added to a solution of the complex, no changes in the relative sizes of peaks in the −14.7 ppm multiplet are observed. We do observe two small, unresolved peaks in the ^{31}P NMR spectrum (P bound to Ir at −40 ppm, broad; P bound to Ag at 11 ppm, broad), which we attribute to a complex that contains a Ag–PPh_3 unit bound outside of the iridium–dimen cage (i.e. a complex with a P–Ir–Ir–Ag–P^{3+} unit). The isolation and characterization of this complex and additional group 1B analogue chemistry will be the subject of a future report.

Acknowledgment. We thank Doyle Britton and Steve Philson for several stimulating discussions and Johnson-Matthey, Inc., for a generous loan of iridium trichloride.

Supplementary Material Available: Tables SI, SII, and SIV, listing crystallographic data, thermal parameters, and intramolecular distances (10 pages); Table SIII, giving observed and calculated structure factors (9 pages). Ordering information is given on any current masthead page.

(19) (a) Carty, A. J.; Graham, N. M.; Taylor, N. J. *J. Am. Chem. Soc.* **1979**, *101*, 3131. (b) Carty, A. J.; Graham, N. M.; Taylor, N. J. *Organometallics* **1983**, *2*, 447. (c) Freeman, M. J.; Green, M.; Orpen, G.; Salter, I. D.; Stone, F. G. A. *J. Chem. Soc., Chem. Commun.* **1983**, 1332. (d) Ladd, J. A.; Hope, H.; Balch, A. L. *Organometallics* **1984**, *3*, 1838. (e) Rhodes, L. F.; Huffman, J. C.; Caulton, K. G. *J. Am. Chem. Soc.* **1984**, *106*, 6874.

(20) A marginally applicable example is described for an organophosphorus compound: Grim, S. O. In *Phosphorus-31 NMR Spectroscopy in Stereochemical Analysis*; Verkade, J. G., Quin, L. D., Eds. VCR Publishers, Inc.: Deerfield Beach, FL, 1987; p 650. To our knowledge, no four-bond, through-metal P–P coupling constants have been observed.

Contribution from the Department of Chemistry and Biochemistry, University of Notre Dame, Notre Dame, Indiana 46556

Direct Determination of the Self-Exchange Rate of a Nickel(IV/III) Bis(oxime–imine) Complex. Investigation of Orientation Effects in Electron-Transfer Reactions

Rosemary A. Marusak, Christopher Sharp, and A. Graham Lappin*

Received February 27, 1990

The electron self-exchange rate for the couple $[Ni^{IV/III}Me_2L(1)]^{2+/+}$ ($Me_2L(1)H_2$ = 3,14-dimethyl-4,7,10,13-tetraazahexadeca-3,13-diene-2,15-dione dioxime) has been determined as 2.4×10^4 M^{-1} s^{-1} at 25 °C and 0.10 M ionic strength by ^{1}H NMR line broadening. Rate constants for cross-reactions calculated with use of this self-exchange rate in the Marcus relationship show good agreement with measured values. The effect of the paramagnetic ions $[Cr(edta)]^-$, $[Ni^{III}Me_2L(1)]^+$, and $[Cr(phen)_3]^{3+}$ on the ^{1}H NMR relaxation rates of the cobalt(III) complex $[Co^{III}Me_2L(1)]^+$ has been used to investigate ion-pair structure in solution. These ion pairs serve as models for the electron-transfer precursor assemblies in the self-exchange reaction and two cross-reactions, respectively. Marcus calculations are relatively insensitive to the precursor structures. However, these structures provide a basis for interpretation of stereoselectivity data.

Introduction

The nickel complex $[Ni^{IV}Me_2L(1)]^{2+}$, where $Me_2L(1)H_2$ = 3,14-dimethyl-4,7,10,13-tetraazahexadeca-3,13-diene-2,15-dione dioxime (I), has a reduction potential[1] of 0.66 V and is a useful outer-sphere electron-transfer reagent.[1-5] Application of the Marcus relationship to cross-reactions with a number of reaction partners leads to estimates for the $[Ni^{IV/III}Me_2L(1)]^{2+/+}$ self-exchange rate from 1×10^4 to 9×10^4 M^{-1} s^{-1}.[4] A pseudo-self-exchange rate has been determined as 6×10^4 M^{-1} s^{-1} from the cross-reaction of $[Ni^{III}Me_2L(1)]^+$ with $[Ni^{IV}Me_2L(2)]^{2+}$, a complex with the structurally similar[3] chiral ligand. In this paper,

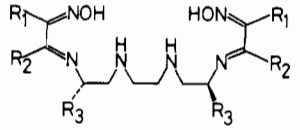

I

$R_1R_2L(1)H_2$ (R_3 = H)

$R_1R_2L(2)H_2$ (R_3 = CH_3)

$R_1R_2L(3)H_2$ (R_3 = $CH_2C_6H_5$)

(1) Lappin, A. G.; Laranjeira, M. C. M. *J. Chem. Soc., Dalton Trans.* **1982**, 1861–1865.
(2) Macartney, D. H.; McAuley, A. *Inorg. Chem.* **1983**, *22*, 2062–2066.
(3) Lappin, A. G.; Laranjeira, M. C. M.; Peacock, R. D. *Inorg. Chem.* **1983**, *22*, 786–791.
(4) Lappin, A. G.; Martone, D. P.; Osvath, P. *Inorg. Chem.* **1985**, *24*, 4187–4191.
(5) Lappin, A. G.; Martone, D. P.; Osvath, P.; Marusak, R. A. *Inorg. Chem.* **1988**, *27*, 1863–1868.

0020-1669/90/1329-4453$02.50/0